JOURNAL OF MATERIALS SCIENCE 13 (1978) 1427–1437

The environmental stress crazing of polycarbonate

J. MILTZ, A. T. DiBENEDETTO, S. PETRIE
Department of Chemical Engineering and Institute of Materials Science, University of Connecticut, Storrs, Connecticut 06268, USA

The environmental crazing from a central hole in extruded polycarbonate sheets, using ethanol as a crazing liquid, was studied. A stress analysis was made to analyse the criteria for craze initiation and growth. The craze length was found to change linearly with the square root of time and the rate of crazing was found to vary exponentially with the applied stress (above a certain stress level). It was concluded that the principal strain is the controlling parameter for environmental craze initiation and growth.

1. Introduction

Since the early studies of Sauer *et al.* [1, 2] and Maxwell and Rahm [3, 4] on crazing of glassy polymers, many thorough investigations in this area have been carried out with the aim of characterizing the structure of the crazes and the parameters controlling their initiation and growth. It is well established now that crazes in glassy polymers are very thin highly oriented porous structures, differing in density and refractive index from the bulk polymer in which they are formed. The question of what is the criterion for craze initiation and growth has been a subject of a long debate in the literature, although it is well known that for a specific polymer, crazing depends on the applied stress, strain, strain rate, temperature, time and environment. It is also known that orientation markedly reduces the propensity of crazes to grow perpendicular to the orientation direction, while parallel to this direction their growth may be enhanced.

Maxwell and Rahm [3] suggested that a critical strain is required before crazing can occur. Critical strains for many glassy polymers have been reported in the literature [3–8]. For polycarbonate a value of 1.8% (in air at room temperature) has been reported [6]. Wang *et al.* [9, 10] conducted experiments in which samples of polystyrene containing a rubber ball (soft inclusion), a steel ball (rigid inclusion) and two rubber balls were subjected to uniaxial tension. From these experiments they concluded that the maximum elastic strain is the controlling criterion for craze initiation. Other investigators have proposed that a critical stress is required to start crazing [11–13], while Kambour [6] states that when homogeneous stress relaxation is not too rapid, critical stress and critical strain criteria can be interrelated through the elastic modulus (i.e., $\sigma_c = E\epsilon_c$). Kambour [14] also suggested that the dilatational component of the stress must be involved in craze initiation recognizing that crazing requires void formation.

As was stated above, crazing is also a time, temperature and strain rate dependent phenomenon. Several investigators have studied craze initiation and growth as a function of these variables [15–17].

Two main hypotheses for the effect of the environment on craze initiation in thermoplastics have been reported in the literature. According to one hypothesis [18, 19] the effect of the crazing solvent is to reduce the energy for craze formation by wetting the surfaces of the polymer. The more accepted hypothesis today [6], first proposed by Maxwell and Rahm [3], is that the effect of the crazing solvent is plasticization and swelling of the polymer thus reducing its T_g and viscosity and allowing flow processes to occur more easily.

As far as craze growth is concerned, most of the works reported in the literature relate the craze length to time, or the rate of crazing (the

change in craze length with time) to the applied stress, strain or strain rate. Regel [17] found a linear relationship between the craze length, l, and log time for PMMA at 20° C:

$$l = K \log (t/t_0) \quad (1)$$

where t_0 is the induction time for craze initiation and K is a constant. Sauer and Hsiao [11, 20] found a linear relationship between the rate of crazing of polystyrene at room temperature and the applied stress, σ:

$$\frac{dl}{dt} = \frac{1}{m}(\sigma - \sigma_0) \quad (2)$$

where σ_0 is the threshold stress for craze initiation (determined by extrapolation to zero growth rate) and m is a constant. They note that at each stress greater than σ_0, crazes appeared immediately upon application of the load, the size of the crazes increasing with increasing load. Thus, for each stress, two growth rates were observed: (a) an initial, very rapid rate, too fast to be detected, (b) a slower, constant rate, after the crazes grow to a small length in the initial stage. Beardmore and Johnston [21] found a linear relationship between the craze length and $(\sigma - \sigma_0)$ in bending experiments of PMMA at 78 K. Higuchi [22] found a linear correlation between the initial growth rate of crazes in PMMA and the applied strain rate, $\dot{\epsilon}$, for a limited range of craze length. Marshall *et al.* [23] have studied the craze growth kinetics of PMMA sheets, containing sharp edge notches, using methanol as the crazing liquid. They used a fracture mechanics approach and expressed their results as a function of the stress intensity factor at the tip of the notch, K_0. They observed three different types of behaviour depending on the level of K_0.

(1) Below a certain value of K_0, designated as K_m, no craze growth occurred.

(2) When K_0 fell between K_m and another, higher value, designated K_n (i.e., $K_m < K_0 < K_n$), craze length increased with the square root of time, suggesting that in this range of K_0 values, craze growth was controlled by the rate of solvent diffusion into the polymer from the end of the crack.

(3) When the value of K_0 exceeded K_n, the crazes grew rapidly at the beginning and then levelled off to a constant crazing rate (increasing with K_0 and sample thickness) which eventually led to fracture. Marshall *et al.* concluded therefore that in this range, the craze growth is controlled by a combination of end flow and side flow of the solvent into the polymer.

Kitagawa and Motomura [24] measured the rate of craze growth in polycarbonate sheet samples. The crazes were initiated from a sharp crack and kerosene was used as the crazing and cracking medium. They obtained non-linear plots of the craze length versus time on a log–log diagram, requiring a viscoelastic model to relate craze length to applied stress and time.

Excellent reviews on crazing and fracture of glassy polymers were given by Rabinowitz and Beardmore [16] and by Kambour [6].

2. Experimental

Plates of Lexan polycarbonate, 8 in long, 4 in wide and 1/8 in and 1/4 in thick were cut from as received extruded sheets, the length being in the extrusion direction. Stress–strain curves of dog-bone shaped samples cut from these sheets revealed that the tensile properties of the material in the machine and transverse directions were almost identical and that the plates for all practical purposes were isotropic. The sides of the plates were polished by 600 grit metallurgical paper and a central hole, of 1/2 in diameter, was milled in the samples. The plates were clamped inside a special tank with glass windows, to allow observation, and loaded to a desired constant load in an Instron testing machine. The crazing solvent (Ethanol 200-proof 100%) was then poured into the tank. The tank was illuminated intermittently from the back by two strong light sources when photographs were taken, at different times, from the front by a 35 mm camera. The slides were then projected onto a screen and the craze length measured as a function of time.

In one of the experiments with the 1/8 in thick sample, the hole was filled with cotton and the solvent applied only through the hole, by frequent injection of the solvent (from a syringe) onto the cotton. In other experiments, a steel cylinder of 1/2 in diameter and of the same length as the thickness of the sample (1/4 in) was glued (by epoxy resin) in the hole. The load and solvent were then applied as mentioned above and photographs taken as time elapsed.

3. Results and discussion

3.1. Craze growth rates

In the present investigation Lexan polycarbonate was studied using ethanol as the crazing environment. The crazes started from a central hole (acting as a stress concentrator). The time scale of the experiments was short enough at the stress levels studied to approximate the polycarbonate sheet as an elastic material.

The stress distribution around a central hole in an infinite elastic plate is given in polar coordinates by [25]:

$$\sigma_r = \frac{\sigma}{2}\left(1 - \frac{a^2}{r^2}\right) + \frac{\sigma}{2}\left(1 + \frac{3a^4}{r^4} - \frac{4a^2}{r^2}\right)\cos 2\theta \tag{3}$$

$$\sigma_\theta = \frac{\sigma}{2}\left(1 + \frac{a^2}{r^2}\right) - \frac{\sigma}{2}\left(1 + \frac{3a^4}{r^4}\right)\cos 2\theta \tag{4}$$

$$\tau_{r\theta} = -\frac{\sigma}{2}\left(1 - \frac{3a^4}{r^4} + \frac{2a^2}{r^2}\right)\sin 2\theta \tag{5}$$

$$\begin{aligned} \sigma_z &= 0 && \text{for plane stress} \\ \sigma_z &= \nu(\sigma_r + \sigma_\theta) && \text{for plane strain} \end{aligned} \tag{6}$$

where σ is the applied stress, a is the diameter of the hole, r is the radial distance from the centre of the hole, θ is the angle relative to the direction of the applied load and ν is the Poisson's ratio of the material.

For a finite plate width, a correction factor should be used with these equations. It can be shown however [25], that for widths equal or greater than 8 times the diameter of the hole (as is the case in the present study) the corrections are negligible. It can be seen from these equations that the maximum stress developed is at the surface of the hole at 90° to the applied load and is equal to $\sigma_\theta = 3\sigma$.

Fig. 1 is a typical plot of the length of the central craze (growing at 90° to the applied load) versus time, for the 1/4 in thickness polycarbonate samples at three different stress levels. Fig. 2 is a plot of the same results on a log–log diagram. Straight lines were obtained with slopes close to 0.5, indicating that the craze growth is controlled by diffusion of the solvent into the polymer through the end of the craze, in agreement with the results of Marshall *et al.* [23] for PMMA.

Fig. 3 is similar to Fig. 2 for the 1/8 in thick samples. Again three parallel straight lines were obtained, but with a higher slope of 0.63. The higher slope suggests that in the thinner samples a combination of end flow and side flow is involved in controlling the rate of craze growth. To confirm this suggestion, an experiment was run in which the solvent was applied only to a piece of cotton which filled the hole and not to the whole sample. In this case no side flow could occur. The lower curve in Fig. 3 shows the results of this experiment. A straight line was obtained but with a slope of 0.48, that is close to 0.5, typical of end flow only. The present results are therefore in agreement with those of Marshall *et al.* [23] for solvent crazing in PMMA. It is worthwhile to

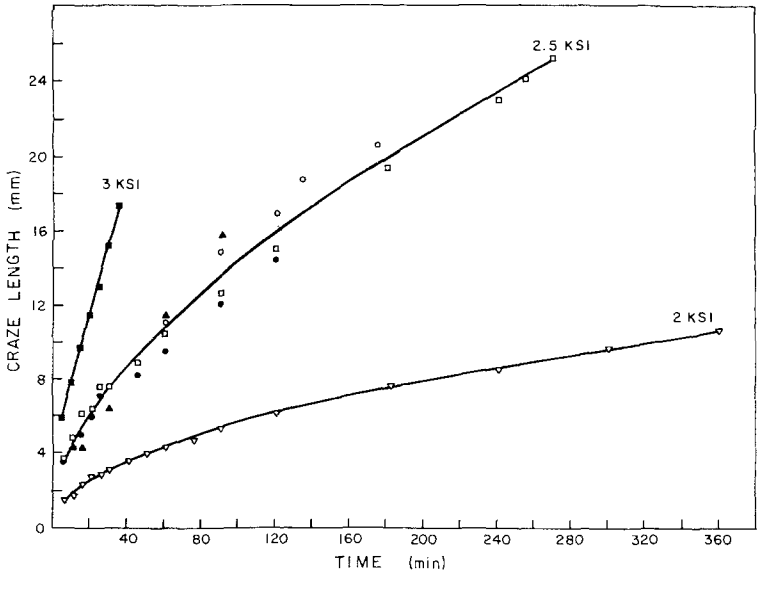

Figure 1 The dependence of craze length on time for the 1/4 in thick polycarbonate samples at three different stress levels.

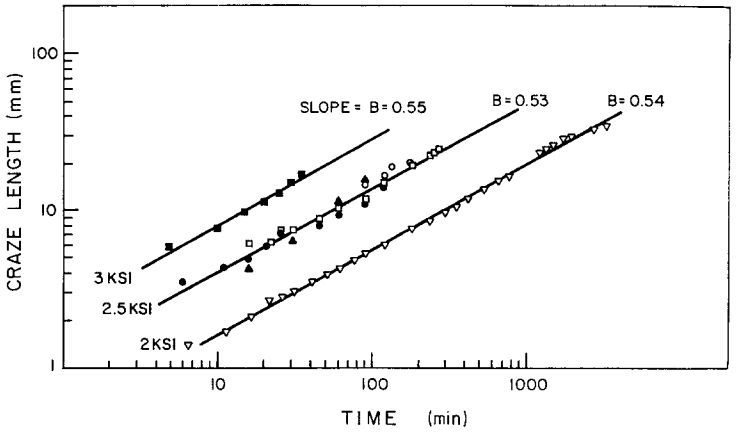

Figure 2 The dependence of craze length on time for the 1/4 in polycarbonate samples. B is the slope of the lines.

mention that in the present study, crazes appeared immediately upon applying the liquid. Our results support, therefore, the suggestion that there are two steps in craze growth, a rapid initiation step followed by a slow growth, as previously reported in the literature [11, 20]. The craze growth in the second step can be described as a function of time by:

$$l = At^n \tag{7}$$

where l is the craze length, A is a stress and temperature dependent parameter (for a specific isotropic polymer–environment system) and the exponent, n, can have values between 0.5 to 1.0 depending on the thickness of the sample. The value of n approaches 0.5 for thick samples and higher values for thin ones. The exact values of "thick" and "thin" probably change from one polymer to another. As the craze length, l, is proportional to t^n, it is clear that the rate of crazing, dl/dt, should be proportional to $1/t^{1-n}$

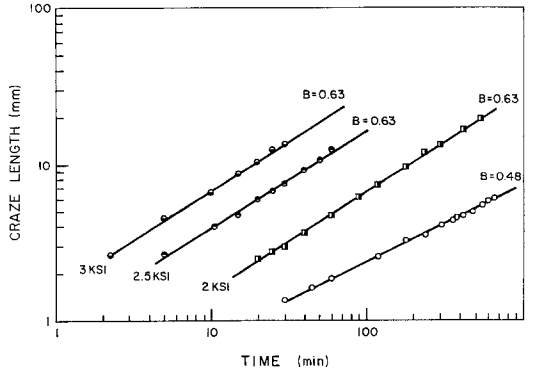

Figure 3 The dependence of craze length on time for the 1/8 in thick polycarbonate samples. In the upper three curves the solvent was applied to the whole sample. In the lower curve the solvent was applied through cotton inside the hole only.

and the following equation could be written:

$$dl/dt = B/t^{1-n} \tag{8}$$

where B is again a stress and temperature dependent parameter (for a given isotropic polymer–environment system).

Fig. 4 is a plot of the rate of crazing at several constant times as a function of the applied stress. Above 2000 p.s.i. parallel lines on a semilogarithmic diagram were obtained, indicating that above

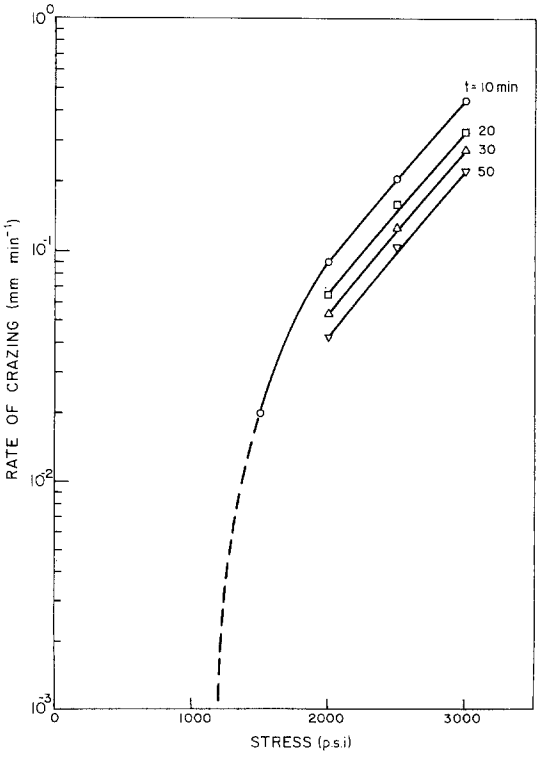

Figure 4 The dependence of rate of crazing on the applied stress at constant times.

this stress level the rate of crazing is exponentially dependent upon the applied stress. This dependence is of the Zhurkov type expression for the lifetime of a body as a function of stress [26]. Similar results were found by Sauer and Hsiao [11, 20] for the crazing behaviour of polystyrene in air. The fact that the lines for different times are parallel indicates that time and stress are separable functions and Equation 13 can be written in the form:

$$\frac{dl}{dt} = \frac{C}{t^{1-n}} \exp(\sigma - \sigma^*) \qquad (9)$$

where C is a temperature dependent parameter (probably also of the exponential type) and σ^* is the threshold stress for craze initiation. In order to check whether a threshold stress exists, experiments were run at stepwise decreasing stresses. While at a stress of 1500 p.s.i. crazes were initiated and continued to grow (although at a very slow rate), at a stress of 1200 p.s.i., very tiny crazes were formed (initial step) which were arrested after a very short craze length. These crazes did not grow during a period of 50 h. It can therefore be concluded that a threshold stress for craze initiation and growth really exists. Taking the theoretical stress concentration factor of a hole as 3, the threshold stress for craze growth in polycarbonate (in ethanol at room temperature) is approximately 3500 p.s.i., corresponding to a critical strain of 1% (cf. 1.8% in air).

3.2. Criteria for craze initiation and growth

Another aspect of crazing studied in the present work was the criterion for craze initiation and the direction of craze growth. Wang *et al.* [9, 10] studied crazing of polystyrene (in air) filled with a steel ball, a rubber ball, and two rubber balls. They showed that with the steel ball, crazes started at the polymer–inclusion interface at an angle of 37° to the applied stress direction, exactly where the principal strain reached its maximum value. They therefore suggested that the principal strain is the controlling parameter in craze initiation. Sternstein *et al.* [27] studied the crazing behaviour of poly(methyl methacrylate) in air around a circular hole. They found three regions in which crazes either did not form at all, or were of uniform density or were very dense. The boundaries between the regions coincided with one of the principal stress contours. They concluded that the principal stress is the controlling parameter in craze formation and that the direction of craze growth is perpendicular to the direction of the principal stress. Bevis and Hull [28] studied the crazing behaviour of polystyrene samples in air, in the vicinity of an edge crack. They plotted the contours of the principal stress and showed that the crazes grew in a direction perpendicular to the major principal stress (or parallel to the minor principal stress). Beardmore and Rabinowitz have shown [29] that in oriented PMMA and polycarbonate samples the craze growth differs in direction from the direction of the minor principal stress.

All the above described studies on the direction of craze growth were carried out in air. To the best of the authors' knowledge, no studies describing the direction of craze growth in the presence of a crazing environment have been reported in the literature. These directions are described and analysed in the present publication.

The principal stresses, in cylindrical coordinates, can be derived from the stresses given in Equations 3 to 6:

$$\sigma_1 = \frac{\sigma_r + \sigma_\theta}{2} + \left[\left(\frac{\sigma_r - \sigma_\theta}{2}\right)^2 + \tau_{r\theta}^2\right]^{1/2} \qquad (10)$$

$$\sigma_2 \frac{\sigma_r + \sigma_\theta}{2} - \left[\left(\frac{\sigma_r - \sigma_\theta}{2}\right)^2 + \tau_{r\theta}^2\right]^{1/2} \qquad (11)$$

$$\sigma_3 = \sigma_z \qquad (12)$$

Calculations based on literature [30] show that for 1/4 in thick polycarbonate samples, plane strain conditions prevail.

To solve for the contours of the principal stress, Equations 3 to 6 can be combined and rearranged to the form

$$8x^2(x^2 - 1)\cos^2 2\theta + 2x^2[2x^2 - 3x^4 + 1 - 4\sigma_1]\cos 2\theta + \{9x^8 - 12x^6 - x^4 + 4x^2 - 4\sigma_1(\sigma_1 - 1)\}^{1/2} = 0 \qquad (13)$$

where $x = a/r$. This is a quadratic equation in $\cos 2\theta$ from which the value of θ is computed for the desired principal stress at any value of x. These values provide the contour of the appropriate maximum stress.

In a similar manner, equations for the contours of the principal strain may be obtained from the corresponding equations for the strains and princi-

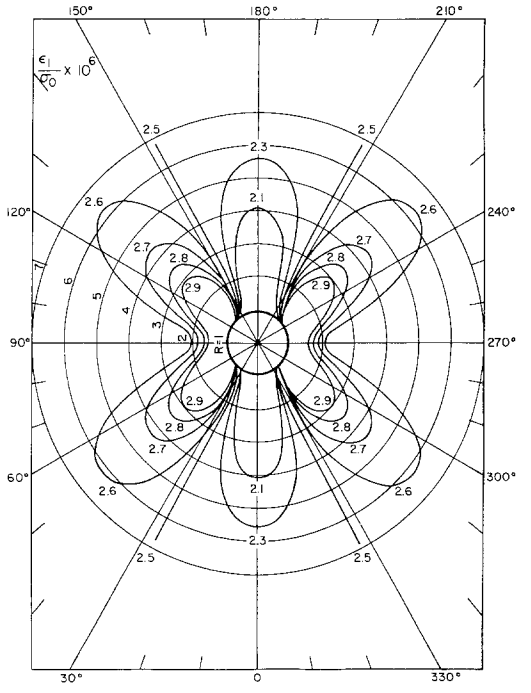

Figure 5 Principal strain contours around the hole (per unit of applied stress).

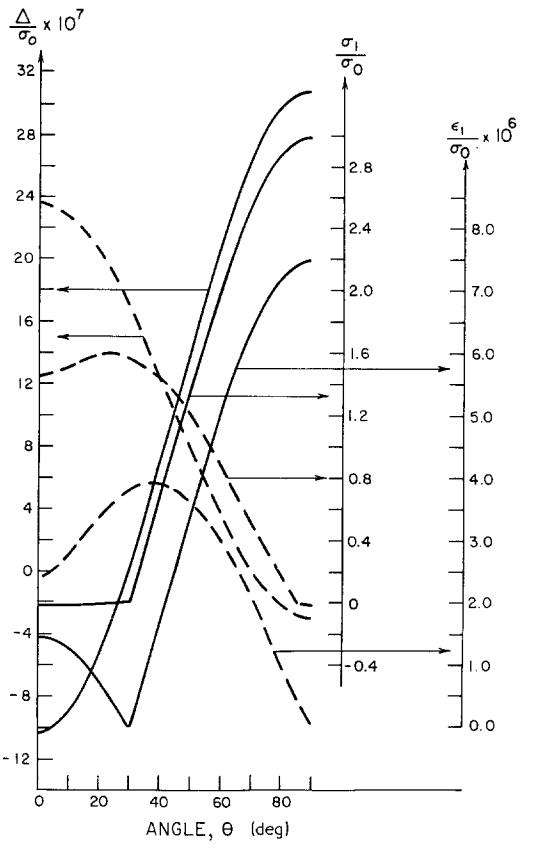

Figure 6 The variation of the major principal stress, principal strain and dilatation with angle. ——— around a hole; – – – – around a cylindrical steel inclusion.

pal strains:

$$8x^2\left[x^2(1-2\nu)(1+\nu)-1\right]\cos^2 2\theta + 2x^2\left[x^2(2-3x^2)-8\nu(1-\nu)+1-\frac{4E\epsilon_1(1-2\nu)}{(1+\nu)}\right]\cos 2\theta + \left\{x^2(9x^6-12x^4-x^2+4) - \frac{4E\epsilon_1}{(1+\nu)}\left[\frac{E\epsilon_1}{(1+\nu)}-(1-2\nu)\right]+4\nu(1-\nu)\right\} = 0 \quad (14)$$

which is again a quadratic equation in $\cos 2\theta$ from which θ can be calculated for a desired strain and any value of x. The values of x and the calculated θ provide the contour of the principal strain. The contours of constant dilatation, Δ, can be calculated in the same manner as described above for σ_1 and ϵ_1.

Fig. 5 illustrates a contour map of maximum strain. The values of the Young's modulus and Poisson's ratio were taken as $E = 345\,000$ p.s.i., $\nu = 0.37$ given by Kazanjian [31]. It can be seen from this figure that for a constant value of x (namely, for a constant distance from the centre of the hole), the principal strain obtains its maximum value at $\theta = 90°$. The same is true for the principal stress and dilatation. This is also shown by the solid lines in Fig. 6 for the change in the principal stress, principal strain and dilatation with the angle in the close vicinity of the hole.

In Fig. 7 the crazes grown from the hole are shown after three different times from the time the ethanol was applied to the stressed sample. It can be seen that the crazes start to grow at $\theta = 90°$ and $\theta = 270°$. Crazes grow also symmetrically in the vicinity of $\theta = 90°$ (and $\theta = 270°$) in the range of $90° - \alpha$ to $90° + \alpha$ (also $270° - \alpha$ to $270° + \alpha$), the value of α depending on the applied load. The higher the load the greater is α. Those crazes grown at $\theta = 90°$ continue to grow in this direction while crazes grown at lower and higher values of θ, curve and tend to bend towards the direction of 90°. After a relatively great distance from the centre of the hole, where the effect of the hole is small, the crazes continue to grow in 90° direction. This craze growth is according to the expectation as all the involved parameters obtain their maximum

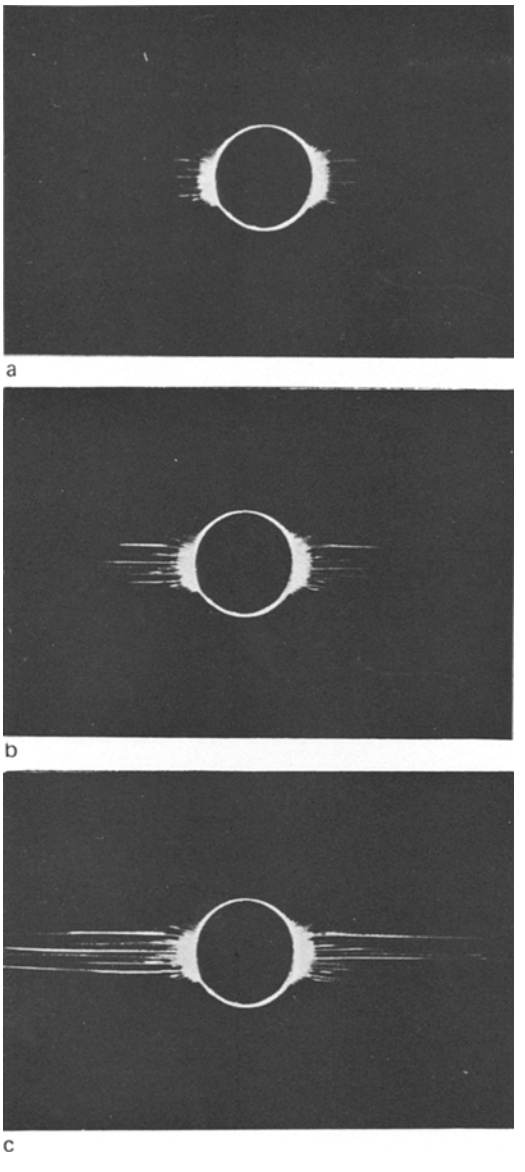

Figure 7 Crazes grown from a hole after, (a) 30 min, (b) 120 min, (c) 240 min.

value at $\theta = 90°$. Sternstein *et al.* [27] have plotted the contours of constant angles of the principal stress and have shown that the direction of the craze growth is perpendicular to this direction. The angle of the principal stress can be calculated from the relation:

$$tg2\delta = \frac{2\tau_{r\theta}}{\sigma_r - \sigma_\theta} \qquad (15)$$

where δ is the angle of the principal stress relative to the radial direction. Fig. 8 is a plot of the contours of constant angles of the principal stress as calculated from Equation 15 and also given by

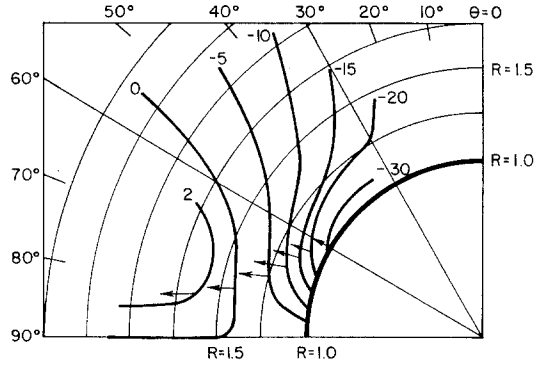

Figure 8 Contours of constant angle of principal strain (and stress), around a hole. The arrows show the direction perpendicular to the direction of the principal strain.

Sternstein *et al.* [27]. As the principal stress, principal strain and dilatation all obtain their maximum value at 90°, it is impossible to conclude which is the controlling parameter for craze initiation. Experiments were therefore run in which a 1/2 in steel cylinder, of the same length as the thickness of the polycarbonate sample, was glued into the hole by an epoxy resin. The load and solvent were applied to the sample in the same manner. The stresses and strains are changed due to the the presence of the solid inclusion. The distribution of the stresses in a plate in the vicinity of a cylindrical inclusion were given by Schuerch [32]:

$$\sigma_r = \frac{1}{2}\left(1 + K_1\frac{a^2}{r^2}\right) + \frac{1}{2}\left[1 - K_2\left(3\frac{a^4}{r^4} - 4\frac{a^2}{r^2}\right)\right]\cos 2\theta \qquad (16)$$

$$\sigma_\theta = \frac{1}{2}\left(1 - K_1\frac{a^2}{r^2}\right) - \frac{1}{2}\left[1 - 3K_2\frac{a^4}{r^4}\right]\cos 2\theta \qquad (17)$$

$$\tau_{r\theta} = -\frac{1}{2}\left[1 + K_2\left(3\frac{a^4}{r^4} - 2\frac{a^2}{r^2}\right)\right]\sin 2\theta \qquad (18)$$

$$\sigma_z = \nu_m\left(1 + 2K_2\frac{a^2}{r^2}\cos 2\theta\right) \quad \text{for plane strain} \qquad (19)$$

For plane strain conditions:

$$K_1 = \frac{E_f(1-2\nu_m)(1+\nu_m) - E_m(1-2\nu_f)(1+\nu_f)}{E_f(1+\nu_m) + E_m(1-2\nu_f)(1+\nu_f)} \qquad (20)$$

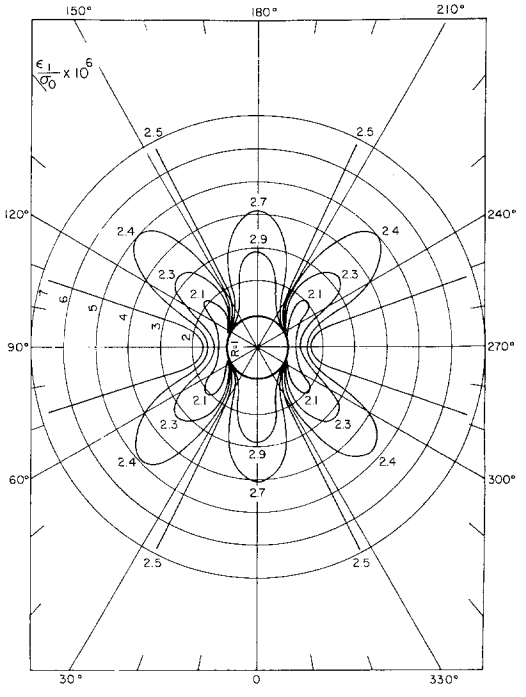

Figure 9 Principal strain contours around a cylindrical steel inclusion.

$$K_2 = \frac{E_f(1+\nu_m) - E_m(1+\nu_f)}{E_f(3-4\nu_m)(1+\nu_m) + E_m(1+\nu_f)} \quad (21)$$

where E_f and E_m are Young's moduli of the inclusion and matrix respectively and ν_f and ν_m are the respective Poisson ratios. The expressions in Equations 16 to 19 are per unit of applied stress. For $K_1 = K_2 = -1$ Equations 16 to 19 reduce to Equations 3 to 6 for a hole. The contours of the principal stress, principal strain and dilatation in the case of the cylindrical inclusion can be derived from Equations 16 to 19 in the same manner as for the hole. The expression for obtaining the contours of the principal strain, for instance, is:

$$\begin{aligned} &4x^2[K_2(2-3x^2) + 4\nu K_2^2 x^2(1-\nu) - K_2^2 x^2] \\ &\cos^2 2\theta + 2x^2\left[K_1(1 - 3K_2x^4 + 2K_2x^2)\right. \\ &\left. + 8\nu K_2(1-\nu) - 2K_2 + 4K_2\frac{E\epsilon_1(1-2\nu)}{1+\nu}\right] \\ &\cos 2\theta + \{x^2[9K_2^2x^6 - 12K_2^2x^4 \\ &+ (K_1^2 + 4K_2^2 + 6K_2)x^2 - 4K_2] \\ &- \frac{4E\epsilon_1}{1+\nu}\left[\frac{E\epsilon_1}{1+\nu} - (1-2\nu)\right] + 4\nu(1-\nu)\} = 0 \end{aligned} \quad (22)$$

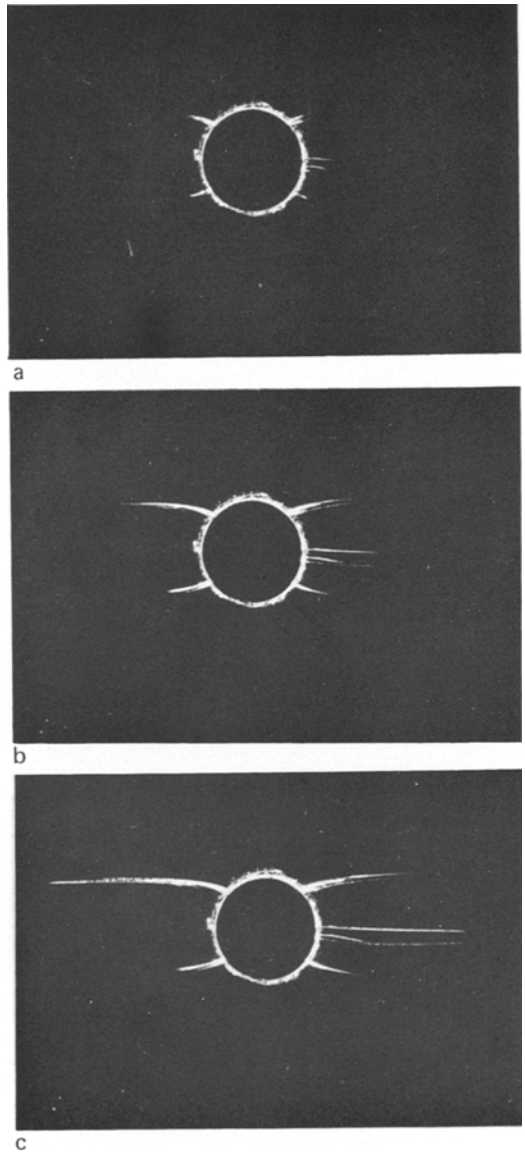

Figure 10 Crazes grown from the polycarbonate–cylindrical steel inclusion interface, (a) after 30 min, (b) after 150 min, (c) after 270 min.

In Fig. 9 the principal strains are plotted in a similar manner as for the hole (cf. Fig. 5), using values of $E_f = 3 \times 10^7$ p.s.i. and $\nu_f = 0.3$. Comparison of Fig. 5 with Fig. 9 shows that although the general shape of the contours have not been changed very much, the distribution of strains has been completely changed. As can be seen from these figures, all the values have been interchanged; that is where the greatest values of strain appeared with the hole, the smallest values appear with the inclusion and vice versa. The same general pattern is followed for principal

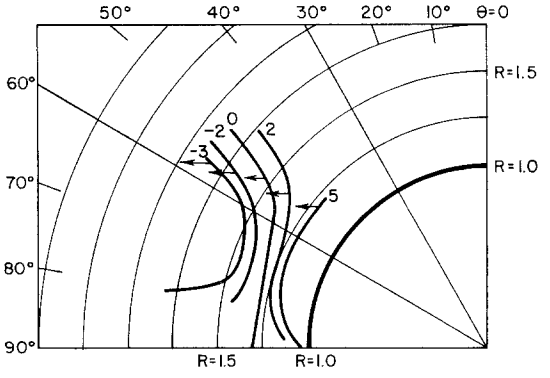

Figure 11 Contours of constant angle of the principal strain (and stress) around the cylindrical inclusion. The arrows point into the direction perpendicular to the direction of the principal strain.

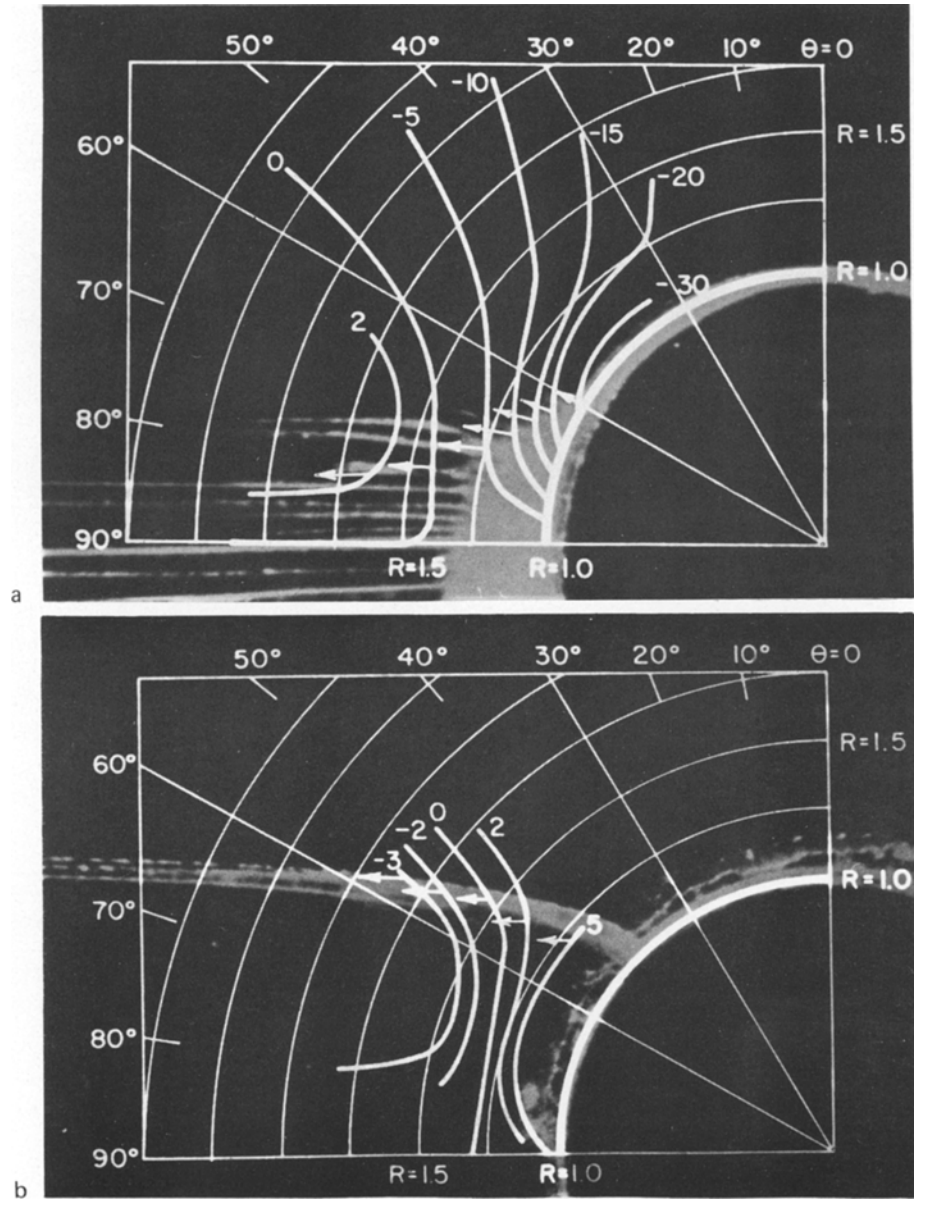

Figure 12 Superposition of the arrows pointing into the direction perpendicular to the direction of the principal strain on the actual crazes, (a) hole, (b) inclusion.

stresses and dilatation. The shift in the values can be seen even better from the dashed curves in Fig. 6. These curves describe the change in the principal stress, principal strain and dilatation with the angle in the close vicinity of the cylindrical inclusion. The principal stress obtains a maximum value at $\theta = 23°$, the principal strain at $\theta = 38°$ and the dilatation at $\theta = 0$. Fig. 10 shows crazes grown from the steel–polycarbonate interface. There is a clear change in the position of craze initiation and in the pattern of craze growth. Symmetrical crazes started to grow at an angle of about 40° with respect to the applied stress which is very close to the angle of maximum principal strain. The two crazes growing at $\theta = 90°$ are probably a result of debonding between the inclusion and the polycarbonate. These results for solvent craze initiation in polycarbonate are the same as obtained by Matsuo *et al.* [10] for the craze initiation in polystyrene with a steel ball inclusion (in air). Moreover, the angle of the principal strain is given by:

$$tg2\Omega = \frac{\gamma_{r\theta}}{\epsilon_r - \epsilon_\theta} \tag{23}$$

where $\gamma_{r\theta}$ is the shear strain. As

$$\gamma_{r\theta} = \frac{1}{G}\tau_{r\theta} = \frac{2(1+\nu)\,\tau_{r\theta}}{E} \tag{24}$$

and

$$\epsilon_r - \epsilon_\theta = \frac{1}{E}[\sigma_r - \nu(\sigma_\theta + \sigma_z)]$$

$$-\frac{1}{E}[\sigma_\theta - \nu(\sigma_r + \sigma_z)] = \frac{1}{E}(\sigma_r - \sigma_\theta) \tag{25}$$

we obtain that

$$tg2\Omega = \frac{2\tau_{r\theta}}{\sigma_r - \sigma_\theta} = tg2\delta \tag{26}$$

which means that at every point, the principal strain and the principal stress have the same direction. The findings of Sternstein *et al.* [27] and of Bevis and Hull [28] that the crazes grow perpendicular to the direction of the principal stress can therefore be also interpreted as the crazes grow perpendicular to the principal strain. As it has been shown however, that the controlling parameter in craze initiation is the principal strain, it is more logical to interpret the observed craze as growing perpendicular to the principal strain. It could have been speculated that at least in solvent crazing, dilatation might be the controlling parameter for craze initiation and growth. The present results however show that this is not the case. The crazes do not initiate at the point of maximum dilatation nor does the growth of the crazes proceed into the region of maximum dilatation. Fig. 11 shows the contours of constant angles of the principal strains (and stresses) in the case of the cylindrical steel inclusion. Comparison of the directions of the arrows in this figure with the direction of craze growth in Fig. 10 show that they are the same. A much more striking comparison between the direction of the arrows in Figs. 8 (for the hole) and 11 (for the inclusion) and the actual direction of craze growth is shown in Figs. 12a and b. In Fig. 12a, Fig. 8 is superimposed on Fig. 7c and in Fig. 12b, Fig. 11 is superimposed on Fig. 10c. It can be seen that the arrows really describe the actual direction of craze growth.

We therefore conclude that the solvent induced initiation and growth of crazes in polycarbonate is controlled by the major principal strain. As basically similar observations were made with PMMA and polystyrene in air [27, 28], the major principal strain is probably the controlling parameter in the initiation and growth of crazes in glassy polymers.

Acknowledgement

The generous support of the General Electric Foundation and the helpful discussion with Dr Roger Kambour are gratefully acknowledged.

References

1. J. A. SAUER, J. MARIN and C. C. HSIAO, *J. Appl. Phys.*, **20** (1949) 507.
2. C. C. HSIAO and J. A. SAUER, *ibid* **21** (1950) 1071.
3. B. MAXWELL and L. F. RAHM, *Ind. Eng. Chem.*, **41** (1949) 1988.
4. *Idem, J. Soc. Plast. Eng.* **6** (1950) 7.
5. E. E. ZIEGLER and W. E. BROWN, *Plastics Technol.* **1** (1955) 341.
6. R. P. KAMBOUR, *Macromol. Rev.* 7 (1973) 1.
7. G. A. BERNIER and R. P. KAMBOUR, *Macromol.* **1** (1968) 393.
8. R. P. KAMBOUR, E. E. ROMAGOSA and C. L. GRUNER, *ibid* 5 (1972) 335.
9. T. T. WANG, M. MATSUO and T. K. KWEI, *J. Appl. Phys.* **42** (1971) 4188.
10. M. MATSUO, T. T. WANG and T. K. KWEI, *J. Polymer Sci. A-2* **10** (1972) 1085.
11. J. A. SAUER and C. C. HSIAO, *ASME Trans.* **75** (1953) 895.

12. G. MENGES and H. SCHMIDT, Conference on Research on Engineering Properties of Plastics, Cranfield, UK (1969).
13. A. N. GENT, *J. Mater. Sci.* **5** (1970) 925.
14. R. P. KAMBOUR, *Polymer* **5** (1964) 143.
15. R. N. HAWARD, B. M. MURPHY and E. F. T. WHITE, *J. Polymer Sci. A-2* **9** (1971) 801.
16. S. RABINOWITZ and P. BEARDMORE, "Critical Reviews in Macromolecular Science", Vol. 1, edited by E. BAER, (CRC Press, Chemical Rubber Co., Cleveland, Ohio, 1972).
17. V. R. REGEL, *J. Tech. Phys. (USSR)* **26** (1956) 359 (English Translation, *Tech. Phys. (USSR)* **1** (1956–57) 353).
18. H. A. STUART, G. MARKOWSKI and D. JESCHKE, *Kunststoffe* **54** (1964) 618.
19. R. L. BERGEN, Jr., *SPE J.* **24** (1968) 77.
20. J. A. SAUR and C. C. HSIAO, *India Rubber World* (1953) 355.
21. P. BEARDMORE and T. L. JOHNSTON, *Phil. Mag.* **23** (1971) 1191.
22. M. HIGUCHI, Proceedings of the First International Conference **2** Sendai, Japan (1966) p. 1211.
23. G. P. MARSHALL, L. E. CULVER and J. G. WILLIAMS, *Proc. Roy. Soc. Lond. A* **319** (1970) 165.
24. M. KITAGAWA and K. MOTOMURA, *J. Polymer Sci., Polym. Phys.* **12** (1974) 1979.
25. S. TIMOSHENKO and J. N. GOODIER, "Theory of Elasticity" (McGraw–Hill, 1951).
26. S. N. ZHURKOV and V. S. KUKSENKO, *Int. J. Fracture* **11** (1975) 629.
27. S. S. STERNSTEIN, L. ONGCHIN and A. SILVERMAN, *Appl. Polymer Symposia* **7** (1968) 175.
28. M. BEVIS and D. HULL, *J. Mater. Sci.* **5** (1970) 983.
29. P. BEARDMORE and S. RABINOWITZ, Craze formation and growth in oriented plassy polymers, Ford Motor Company, Scientific Staff Report No. SR-71-122.
30. ASTM E-399-74.
31. A. R. KAZANJIAN, *Polymer–Plast. Technol. Eng.* **2** (1973) 123.
32. H. SCHUERCH, "Proceedings of the Fiftth Symposium on Naval Mechanics" edited by F. W. Wenat, H. Liebowitz and N. Perron (Pergamon Press, 1970) p. 586.

Received 27 June and accepted 5 October 1977.